Microstructure-based Description of the Deformation of Metals: Theory and Application

Dirk Helm, Alexander Butz, Dierk Raabe, and Peter Gumbsch

Aiming for an integrated approach to computational materials engineering in an industrial context poses big challenges in the development of suitable materials descriptions for the different steps along the processing chain. The first key component is to correctly describe the microstructural changes during the thermal and mechanical processing of the base material into a semi-finished product. Explicit representations of the microstructure are most suitable there. The final processing steps and particularly component assessment then has to describe the entire component which requires homogenized continuum mechanical representations. A key challenge is the step in between, the determination of the (macroscopic) materials descriptions from microscopic structures. This article describes methods to include microstructure into descriptions of the deformation of metal, and demonstrates the central steps of the simulation along the processing chain of an automotive component manufactured from a dual phase steel.

INTRODUCTION

Industrial success in materials related technologies relies on the possibility to specifically engineer materials and products with improved performance. The key success factor is the ability to make these developments timely and at relatively low cost. This demands not only the rapid development of new or improved processing techniques but also better understanding and control of material structure, performance, and durability. Such control of materials involves multiple length and time scales and multiple processing stages or the coupling of processing and performance assessment. To achieve this,

How would you…

…describe the overall significance of this paper?

The paper gives an overview of different strategies to include the polycrystalline microstructure into the description of the deformation of metals. It discusses the integration of results from computational multi scale materials engineering into practical industrial applications. A process chain simulation of sheet metal components is used to illustrate the current state of the art.

…describe this work to a materials science and engineering professional with no experience in your technical specialty?

In this paper, numerical approaches are discussed to represent the microstructure evolution and the resulting effective properties of polycrystals and multiphase metallic materials. The results of the micro scale simulations are used to numerically model the process chain of a sheet metal component under consideration of the results from the previous process step.

…describe this work to a layperson?

The article describes different simulation methods to predict the evolution of the material properties of metals due thermal or mechanical processing. This knowledge is of high importance since this change of material properties typically occurs during the different process steps from a semi-finished part to the final component. Providing appropriate simulation tools allows virtually to develop and optimize the production process and to reduce cost and time consuming "trial and error" test. This simulation approach is illustrated for the production process of a sheet metal component for application in automotive industry.

the materials descriptions and the flow of information necessarily have to be based on materials microstructure characteristics. Such inclusion of materials specifics in engineering simulation still is one of the major challenges for the development of improved materials modeling and simulation.[1,2]

The linkage between materials microstructure and materials properties is at the heart of materials modeling in general but very specifically so for the description of materials deformation. Multiscale approaches (Figure 1) are required to make the link from the discrete dislocations, grain and phase boundaries which constitute the materials microstructure, to the continuum plasticity descriptions appropriate at larger scales. While it may certainly be appropriate to investigate micro-components directly at the level of discrete defects, like the dislocation dynamics investigations of thin films,[3,4] micro-pillars[5] or micro-bending bars,[6] large scale components mandate the final treatment of the component in a continuum mechanical framework.[7] Although there have been many attempts to include the discrete dislocation behavior rigorously in continuum mechanical materials modeling,[8] the mathematical frame for such inclusion has only recently been developed[9,10] and is still far from being applicable. Consequently, the materials models are either effective materials descriptions or have come to be physically based to at least include some direct microstructural information. Similarly it is neither desirable nor intended to include the grain or phase morphology of a material explicitly in the materials modeling at large scale. One therefore either uses effective representations of texture or homogenization techniques to arrive

at continuum mechanical models. The first part of this manuscript describes these different modeling techniques for the continuum mechanical modeling of plastic deformation in single and poly-crystalline materials.

In the second part of this manuscript, the applicability of modern microstructure-based modeling in industrial forming simulations is assessed.[11] The drive toward microstructure-based models comes, on one hand, from process simulation and the optimization of individual processing steps or the entire processing chain during manufacturing and, on the other hand, from the requirement of higher precision in the simulation of component manufacturing and component assessment. Figure 2 pictorially displays such a processing chain and the final component assessment.

Today, microstructure-based simulations are used, for example, in the process simulation of semi-finished parts in the aluminum industry.[12] This aids process optimization and the specific adjustment of materials properties of the sheet material. For aluminum, alloy development and the individual processes determining the microstructure are reasonably well understood and modeling is developed to a relatively high level.[13] Other materials, and particularly the steels, are less well understood and detailed microstructural modeling is still rare. This is in part due to the many complex phase transformation phenomena and kinetic pathways involved.[14,15] In the overall component design, which involves an assessment of the crash worthiness of automotive components, or even the shape, springback or property predictions of components out of the deep drawing and stretching steps, microstructural modeling is basically not yet employed. However, the perspectives for microstructure-based modeling in this field are great. It can, for example, correctly represent the anisotropic yield surface and its non-uniform evolution during deep drawing and thereby not only enable much more precise prediction of the local properties of a component but also allow for integrated product optimization through the entire process chain. As an application example of such integral materials modeling

we report here simulations of the final steps in the processing chain of a dual phase carbon manganese steel sheet, which is intended for use in automotive components.

CRYSTAL PLASTICITY

During the last decades, extensive experimental investigations on single crystals and the evolved physical knowledge about the occurring deformation mechanisms in metals has stimulated the development of appropriate constitutive theories in the framework of continuum mechanics. The continuum mechanical representation is restricted to suitable problems but at the same time the best way to represent certain parts of a complex process chain. An important ingredient when aiming at through-process models is the use of internal variable constitutive formulations that are capable of tracking history dependent behavior. Typical internal variables are dislocation density, grain size, and second phase dispersion. The use of external variables (such as strain) cannot describe inheritance of microstructures through a sequence of processes.

Finite Strain Single Crystal Plasticity

Kinematics

The kinematics of finite deformation[16] describes a situation where a material point that is originally in a reference configuration is deformed to the current state by a combination of externally applied forces. The local changes in space are given by the deformation gradient, which transforms tangent vectors on material lines from the reference configuration in tangent vectors of material lines in the current configuration (Figure 3). In order to distinguish between elastic and plastic deformations, the idea of Kröner[17–19] to incorporate a multiplicative decomposition of the deformation gradient into an elastic and plastic part is nowadays well established: The elastic part results from the reversible response of the lattice to external loads and displacements including rigid-body rotations while the plastic part of the deformation gradient is an irreversible permanent deformation that persists when all external forces and displacements

are removed. In this sense, transformation of the reference state by the plastic part of the deformation gradient leads to an intermediate configuration which is free from external stresses and which is generally considered to maintain a perfect lattice (Figure 4). The velocity of each material point of a body in motion forms a vector field measured in the current state. The spatial gradient of this velocity field describes the change in time of tangent vectors on material lines in the current configuration. The previously introduced multiplicative decomposition of the deformation gradient leads to an additive decomposition of the spatial velocity gradient into an elastic and plastic part. In general, the plastic part is influenced by elastic deformations. However, if the velocity gradient is expressed on the intermediate configuration, the resulting plastic part depends only on plastic deformations.

In the case of dislocation slip, the plastic part of the deformation gradient on the isoclinic intermediate configuration can be formulated as sum of the shear rates on all slip systems. The idea behind the isoclinic intermediate configuration is that the slip vectors and the normal vectors have the same orientation in the reference configuration and the intermediate configuration. Consequently, the rotational part of the plastic part of the deformation gradient is fixed and therefore only the push forward to the current configuration leads to changes in the orientation of the material substructure in form of the crystal lattice (Figure 4).

In addition to the dislocation slip, mechanically driven displacive transformations (i.e., twinning and martensitic phase transitions) play an important rule in many metals (magnesium, titan, modern steel grades like TRIP- and TWIP-steels, etc.). In general, there are several ways to incorporate the displacive transformations in the kinematics of crystal plasticity. The displacive transformations are incorporated in the form of additional slip systems[20–23] or by using a multiple multiplicative decomposition of the deformation gradient,[23,24] which consists of an elastic and plastic part and an additional part for representing the transition. Due to this, an additional intermediate configura-
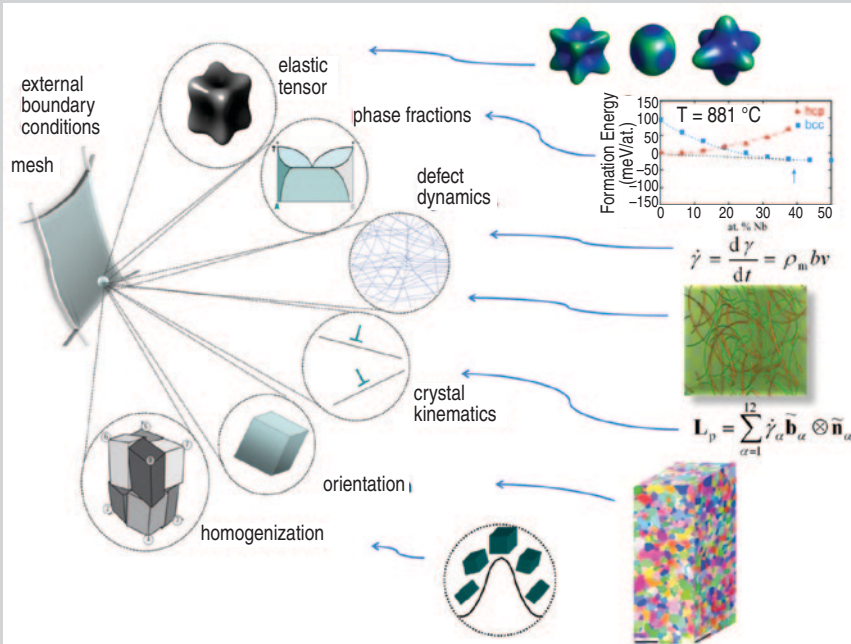
Figure 1. Scheme of a continuum mechanical framework for polycrystal-polyphase mechanics with various ingredients describing the material behavior indicating various options for choosing the adequate degree of microstructure coarse graining and homogenization.
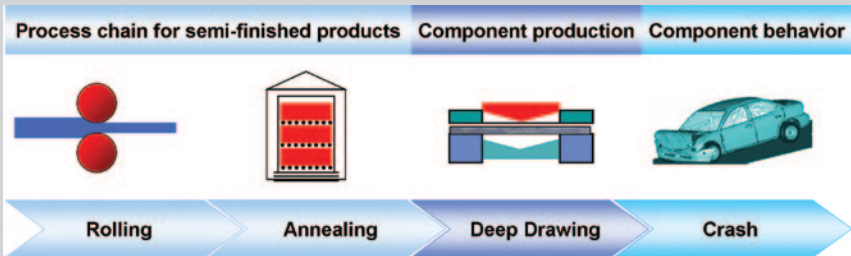
external boundary conditions
mesh
elastic tensor
phase fractions
defect dynamics
crystal kinematics
orientation
homogenization

$T = 881\,°C$

Formation Energy (meV/at.)

$\dot{\gamma} = \dfrac{d\gamma}{dt} = \rho_{m} b v$

$\mathbf{L}_p = \sum_{\alpha=1}^{12} \dot{\gamma}_\alpha \, \tilde{\mathbf{b}}_\alpha \otimes \tilde{\mathbf{n}}_\alpha$

Process chain for semi-finished products | Component production | Component behavior

Rolling | Annealing | Deep Drawing | Crash

Figure 2. Process chain from the hot rolled sheet to the crashed part.

Reference configuration | Current configuration
Deformation gradient **F**
Tangent vector on a material line $d\boldsymbol{X}$
Tangent vector on a material line $dx = \mathbf{F}d\boldsymbol{X}$
Position vector $\boldsymbol{X}$ of the material point $\boldsymbol{P}$
Position vector $x = \chi(\boldsymbol{X},t)$ of the material point $\boldsymbol{P}$
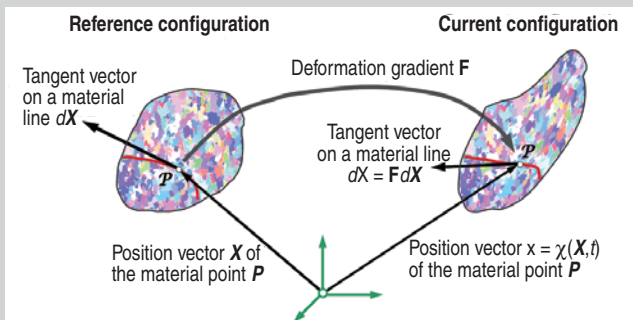
Figure 3. Representing finite deformations in the framework of continuum mechanics.

Isoclinic intermediate configuration
Slip normal
Plastic part of the deformation gradient $\mathbf{F}_p$
Elastic part of the deformation gradient $\mathbf{F}_e$
Slip direction
Current configuration
Slip normal
Slip normal
Reference configuration
Slip direction
Deformation gradient **F**
Slip direction

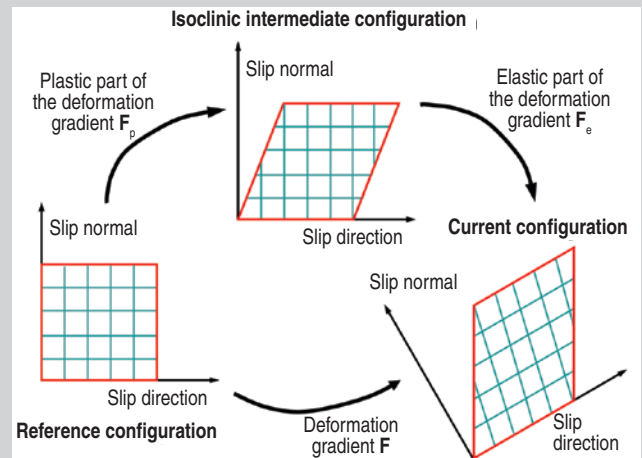Figure 4. Representing finite plastic deformations by means of a multiplicative decomposition of the deformation gradient.

Taylor model | RGC scheme
Color map: Equivalent total strain

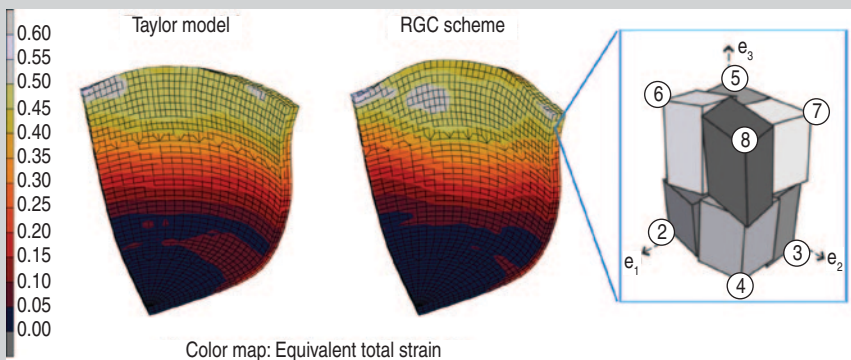0.60 0.55 0.50 0.45 0.40 0.35 0.30 0.25 0.20 0.15 0.10 0.05 0.00

Figure 5. Right hand side: Example of a grain-cluster approximation (RGC[56]) where the constraints are placed on the corners of the aggregate while internal relaxations are admitted; left hand side: two simulation runs using two different homogenization models. (Photo courtesy of D. Tjahjanto)
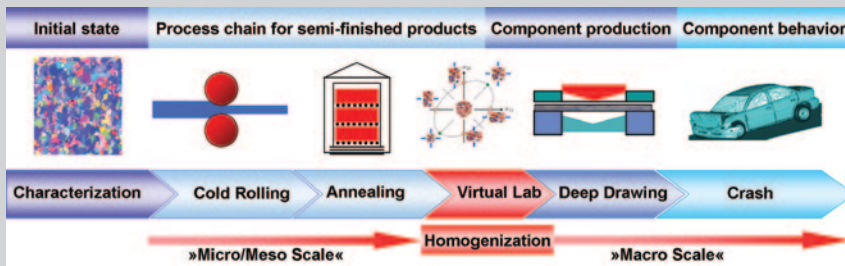
Figure 6. Modeling strategy for representing the process chain for sheet metal production.
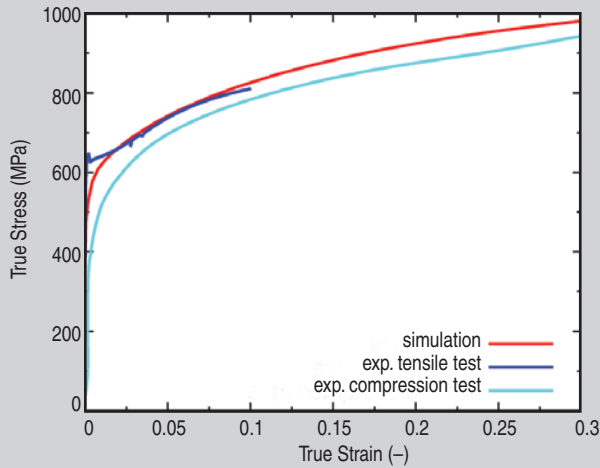

Figure 7. Tensile test on the hot rolled sheet. Comparison between experimental data and the calibrated microstructure model.
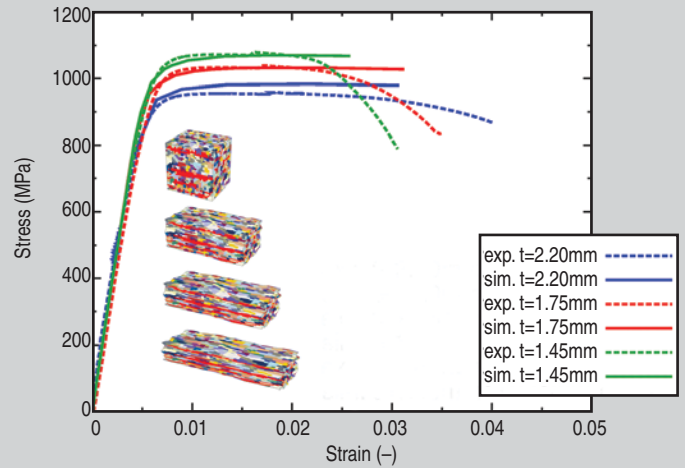

Figure 8. Tensile tests on the (hard, as rolled) cold rolled sheet (hard as rolled) for different degrees of rolling. The initial thickness of the hot rolled sheet is 3.5 mm.
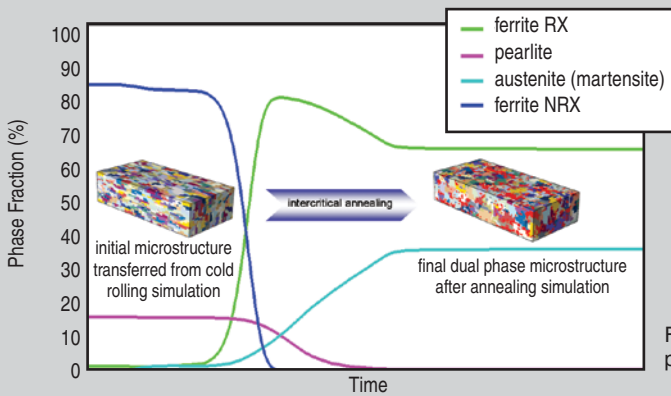

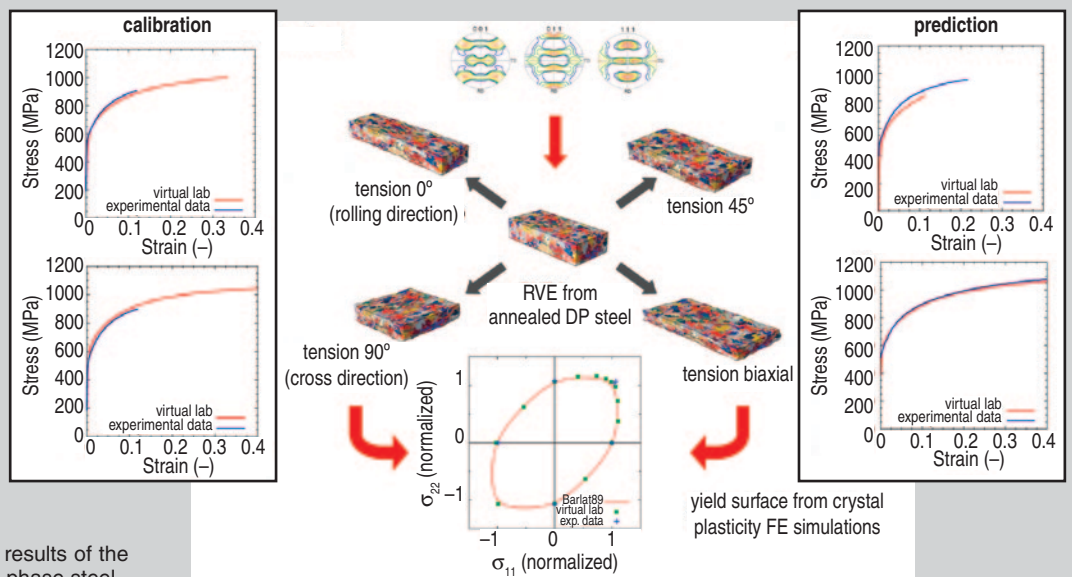Figure 9. Simulation of the microstructure evolution during the annealing procedure.

Figure 10. Application and results of the virtual laboratory on a dual phase steel.

tion arises.

Finally, it is worth mentioning that the sketched kinematic relations for representing the plastic deformations are identical for both phenomenological and physical based models.

Phenomenological Constitutive Models

Based on the kinematical relations for modeling the main deformation mechanisms in metals, different types of phenomenological models for representing crystal plasticity can be introduced. The most important constituents are the elasticity relation, the constitutive equations for representing the kinetic of slip or transition processes and the hardening behavior.

The anisotropic elastic behavior of crystalline structures can be incorporated by hypoelasticity,[25] Cauchy elasticity,[21,26] or hyperelasticity.[16] As long as the elasticity relation does not possess a strain energy function, as in the case of many hypolelastic formulations, it has been well discussed in the literature[27] that energy dissipation occur if closed cycles of deformation are considered. This is a strong disadvantage of such elasticity relations.

So far, the kinematic relation (Figure 4) describes only the geometrical aspects of the evolving plastic anisotropy. In addition, the kinetic of the plastic deformation on the glide systems (i.e., the shear or slip rate) must be defined. Due to the physical understanding, the shear rate on a slip system depends mainly on the resolved shear stress on the slip system and is often influenced by deformation rates. For representing the slip and in particular the slip rate,[28] concepts in the framework of viscoplasticity with yield limit[16,29] and without yield limit,[25,30] has been proposed and applied. In contrast to rate-independent plasticity models, the current yield point is influenced by the deformation rate.[28] Independent on which formulation is preferred, the relation between the resolved shear stress on the slip system in relation to the critical stress is the most important quantity for the amount of plastic slip.

In phenomenological theories, the evolution of the critical resolved shear stress is modeled by means of history dependent internal variables. Mostly, the strain hardening behavior is rep-

resented as a function depending on the accumulated slip.[25,31] While this allows for the description of fundamental hardening phenomena including tension-compression asymmetries in basal textured magnesium alloys by means of a suitable twinning model,[20] the modeling of some anisotropic hardening phenomena like the Bauschinger effect requires additional internal variables, i.e. back stresses on the slip system.[16,29,32]

The deformation of metals depends strongly on temperature and is accompanied by dissipation phenomena. From this point of view, modeling in the framework of continuum thermodynamics leads to valuable insights. In such thermodynamic frameworks,[16,24,29,33] the energy storage phenomena are modeled by using a thermodynamic potential like a free energy function, which depends on the temperature, the elastic part of the deformation gradient, and internal variables. The evaluation of the Second Law of Thermodynamics leads to potential relations for the stress tensor and the entropy as well as a remaining dissipation inequality, which must be fulfilled by the evolution equations for the internal variables. For example, an important consequence of such finite strain thermodynamic considerations is that the projection of the Mandel stress tensor[18] on the glide system in the isoclinic intermediate configuration is the driving stress for occurring slip.

Physically Based Models

In contrast to conventional viscoplastic hardening models, physically based constitutive formulations use internal variables that describe the material state and its history in terms of microstructure parameters. In the case of plasticity the most relevant microstructural state variable is the dislocation density.

When using dislocation-density based constitutive models, the individual shear rates on each glide system, expressed by the plastic part of the velocity gradient tensor, are coupled via the Orowan equation to the underlying density of mobile dislocations that carry this shear rate. The evolution of the total dislocation density (including both, mobile and immobile disloca-

tions) is described through a set of rate formulations that quantify annihilation, multiplication, immobilization, and mobilization events on each individual slip system in a statistical manner. Depending on the specific model design different types of dislocation classes can be defined together with their respective evolution equations and activation barriers reflecting the underlying dislocation processes. Typical examples are the use of edge versus screw dislocation kinetics or the use of dislocations in cell walls and in cell interiors. Details about such formulations and comparisons with experiments can be found in References 23 and 34.

Further parameters for characterizing the microstructure are for instance the grain size, second phase fractions, and precipitates. Some of these parameters (grain size, precipitates) can enter for instance into the mean free path equation for the mobile dislocations or as constants that quantify the increase in friction stress as a function of composition (solutes). Alternatively, grains can be treated individually, where each grain is represented by a set of integration points of identical initial crystal orientation.

High second phase fractions above about 10 vol.% can be considered either in from of a full-field approximation where different phases occupy different finite elements or in an averaged form where the stress response from a two-phase assembly at one integration point is calculated by a separate homogenization model.

The use of physically based models is particularly relevant for precise stress, shape, and texture predictions for forming at small scales,[35–37] under complex loading paths, for damage initiation,[38] for Bauschinger effects,[39,40] and for the behavior of instable texture components.[41] Fine details of the constitutive laws are less essential for simulating large scale forming problems with simple loading paths and microstructure history.

Representing the Behavior of Polycrystals

Polycrystalline and also multiphase metallic materials are of particular interest in technical applications. In this situation, the inhomogeneity in the

microstructure due to texture, precipitations, different phases, etc. requires suitable homogenization schemes for the transition from single crystals to polycrystals.

Mean-field Methods

A reasonable way to obtain the effective properties of a material is given by homogenization schemes on the basis of simplified assumptions about the material behavior and the morphology of the microstructure. In such mean-field approaches the microstructure can be considered as a system of an inclusion that is embedded in a matrix. The most basic assumptions would be either uniform stress or uniform deformation gradient among all phases or respectively grains present in the microstructure. These cases were suggested by Reuss[42] and Voigt[43] for elasticity. The fully constrained Taylor[44] model for plasticity or the extension of Lin[45] for elasto-plasticity correspond to the uniform strain assumption. Both assumptions ignore the shape and specific local neighborhood of the inclusions and generally violate strain compatibility and stress equilibrium, respectively. More sophisticated mean-field assumptions make use of the Eshelby-solution[46] to the problem of an elastic ellipsoidal inclusion in an infinite elastic matrix.

Out of those, the most frequently employed are the self-consistent approach originally suggested by Kröner,[47] and the scheme introduced by Mori and Tanaka.[48] In the former method, each inclusion is treated as isolated within a matrix having the unknown integral stiffness of the compound. The latter approach embeds each inclusion into the original matrix but considers the average matrix strain to act as far-field strain on the overall composite. However, extension of such homogenization schemes from the linear to the non-linear case faces difficulties, most significantly because the stiffness (i.e., strain(rate)-sensitivity of stress) is typically inhomogeneous for a given phase due to its heterogeneous strain. The stiffnesses are usually homogenized by using the average strain per phase as a reference input into the respective constitutive law. In order to establish a link between stress and strain per

phase, secant (connecting total stress to total strain) and tangent (connecting stress increments to strain increments) formulations for the moduli are employed.[49] As an example, the viscoplastic self-consistent mean-field approach (VPSC) has been successfully applied to represent the texture evolution in different types of polycrystalline metals: zirconium alloys,[49] TWIP-steels,[50] and tungsten.[51] Recent developments incorporate elasiticity in the model[52] enabling a more accurate description of the material behavior.

An alternative set of mean-field polycrystal approaches are the grain-cluster models. They represent an intermediate approach between the mean-field schemes and full-field solutions. They reduce the high computational cost of the latter by restricting the degrees of freedom to a small number of regions with (typically) homogeneous strain inside each region. Those areas are grains or phase, thus extending the mean-field approaches by taking into account direct neighbor–neighbor interactions among the constituents of a polycrystalline and potentially also multiphase aggregate. The introduction of grain aggregates allows relaxation of the assumption of homogeneous strain in each constituent (Taylor)—which generally led to an overestimation of the polycrystalline strength and rate of texture evolution—by enforcing compatibility only in an average sense for the aggregate as a whole. Typical examples of such models were suggested by Van Houtte,[53,54] Gottstein,[55] and Eisenlohr[56] (Figure 5). The reasonable numerical effort for solving mean-field problems enables the coupling of the homogenization schemes in finite element algorithm,[7,56–58] for solving more complex initial boundary value problems like the deep drawing of a cup (see Figure 5) or study the texture evolution during rolling.[57]

Full-field Methods

Full-field models of crystal mechanics pursue strategies for solving initial boundary value problems of polycrystalline unit cells. In contrast to the mean-field methods, full-field methods provide a more realistic representation of the stress and strain state in each grain and also the accompanied gradi-

ents, along with an accurate description of the grain morphology, an improved quantitative description of the texture, and a reasonable representation of the interaction between the considered constituents (i.e., grains, phases, etc.). Most of the current numerical treatments of the full-field homogenization schemes are based on the finite element method. Examples on this approach were given by References 29, 59–61 for material science applications as well as References 22 and 62 for simplified bulk metal forming processes like rolling and wire drawing. Without appropriate strategies such full-field approximations are usually too time consuming for applications in through-process modeling. To remedy this problem fast Fourier transform (FFT) based methods can be applied.[63] In comparison to the high computational demand of FE based methods, FFT based full-field solutions require much less computer times.[64]

APPLICATION OF MULTISCALE MODELS FOR SOLVING ENGINEERING PROBLEMS

Virtual Laboratory

In the industrial practice of simulating complex forming operations, the prediction of exact shapes, material flow, thinning, wrinkling, earing, and springback effects is a challenge, particularly when materials with complex textures and microstructures are involved. In the simulation packages that are currently in commercial use, for instance, in the automotive industry, only empirical constitutive laws are available. As these formulations provide only limited empirical access to the material anisotropy and heterogeneity they do not properly take into account the effects of microstructure and texture and their evolution during deformation. The crystal plasticity finite element method (CPFEM) bridges the gap between the polycrystalline texture and macroscopic mechanical properties and opens the path to a more profound consideration of metal anisotropy in commercial forming and process simulations.

The example presented in this section is an application of the CPFE method for the concept of virtual mate-

rial testing (virtual laboratory) using a representative volume element (RVE) approach. By using such numerical test protocols it becomes possible to determine the actual shape of the yield locus as well as corresponding anisotropy coefficients (i.e., Lankford parameters, r-values) directly through CPFE simulations, and to use this information to calibrate empirical constitutive models used, for example, in the automotive industry. Along with standard uniaxial tensile tests, other strain paths can be simulated, such as biaxial tensile, compressive or shear tests. The analysis of loading condition which can not be realized experimentally (like biaxial compression of sheet metal) is also of interest to extend the experimental available data. For practical application, the homogenized results obtained from the virtual lab can be processed in the same manner as conventional experimental results. In the present example the use of the CPFE method for virtual testing is demonstrated for a dual-phase C-Mn steel grade where the parameters of an empirical yield surface function were calibrated by the full-field crystal plasticity predictions (Figure 10).

Representation of Process Chains

While simulation solutions for single process steps are applied successfully to virtually study the ability to process or service parts, a unified approach that reuses knowledge and results from previous steps along the production chain is still an exception. Especially the gap between numerical steel design and corresponding simulation techniques in sheet metal forming and crash simulation is a challenging topic for industrial applications.

In this example,[65] a process chain simulation is presented that covers the consecutive stages of production of a dual phase steel DP800 material. It starts with the hot rolled strip which is followed by cold rolling, heat treatment, deep drawing and finally the analysis of the crashworthiness of the deep drawn component. An important aspect to take into account is the microstructure evolution during the different process steps for an appropriate modeling of the material behavior.

Depending on the process step, different simulation strategies on different length scales are applied (Figure 6).

The first process step to be simulated is cold rolling. Here, a full field simulation approach (RVE) in combination with a CPFE model is used. Different experimental analysis procedures were carried out to account for the initial state of the hot rolled sheet material. Micrographs were used to analyze the ferritic-pearlitic microstructure. To obtain a realistic distribution of the pearlite phase within the ferrite matrix, a statistical reconstruction scheme based on Reference 66 was applied. EBSD data are used to consider a realistic initial texture. Finally, the parameters of the single crystal plasticity material model are calibrated using macroscopic tensile and compression tests (Figure 7).

A prescribed deformation was applied on the RVE-model to simulate the cold rolling process. Three different degrees of rolling were considered with final sheet thicknesses of 2.20, 1.75 and 1.45 mm. According to real tensile test on the as rolled material, similar virtual tests were performed on the rolled RVE-models. Figure 8 shows the very good agreement between the tensile test and the prediction of the model. The hardening behavior can be predicted independently from the applied deformation.

During the subsequent thermal treatment the final dual phase steel microstructure composed of ferrite and martensite is obtained. The corresponding simulation (Figure 9) aim at describing the microstructure change (phase transition, recrystallization and recovery) due to the annealing procedure. The simulation of the thermal treatment is carried out by a cellular automaton.[67] The morphology of the cold rolled RVE model is mapped onto a regular grid. Data concerning the grain number, the orientation of the crystal lattice and the accumulated plastic strain were provided from the rolling simulation to define the initial state for the annealing simulation. The accumulated plastic strain is used to estimate the dislocation density which acts as a driving force within the annealing simulation.

For practical application of deep drawing simulations, models which directly consider the microstructure are

not appropriate due to the high numerical cost and the complexity of the material description. Usually, deep drawing simulations are continuum-based which describe the yielding and hardening behavior with phenomenological models. For this reason, the obtained data from the annealing simulation were homogenized using the virtual lab as described in the preceding section. The obtained macroscopic uniaxial stress-strain curves are used—similar to experimental data—to adjust the parameter of the phenomenological plasticity models. Here, the Barlat89[68] yield function is applied to describe the initial yielding of the dual phase steel. In Figure 10 this procedure is illustrated. The yield points obtained from the virtual lab and the Barlat89 yield locus which is calculated from experimental data do agree very well. Depending of the number of virtual tests, more complex yield functions with more parameter can also be fitted. After the determination of the material behavior by means of the virtual laboratory, the resulting material parameters are used to calibrate macroscopic models for complex deep drawing simulation.[69]

Finally, the crashworthiness of the deep drawn component is virtually analyzed. To obtain accurate failure predictions, the load history from the previous deep drawing process is considered. Therefore, the local thinning of the sheet and the actual hardening of the material at the end of the deep drawing simulation is mapped to the crash simulation.[70]

CONCLUSIONS

From an initial microstructure, the cold rolling of the initial ferritic-perlitic microstructure of a C-Mn steel sheet was evolved in a CPFE simulation to give the texture changes and a grain-specific deformation. This information was sufficient to feed the simulation of the recrystallization processes during heat treatment. With the dual phase microstructure after recrystallization, virtual testing of the deformation behavior was performed. This required two simple calibration experiments but then nicely predicted multiaxial deformation behavior. In the subsequent deep drawing and crash simulations one then has access to local changes in

the mechanical properties of a component, which goes far beyond classical component analysis.

On the basis of appropriate numerical treatments, the discussed constitutive theories are able to represent the microstructure evolution and the resulting effective properties of complex polycrystalline and also multiphase metallic materials. This results in a deeper insight into the process and the interactions between the process steps. This knowledge will help to optimize individual process steps and also to improve the complete process chain. Once established, the modeling along the processing chain allows for both virtual process development and component assessment in unprecedented detail and with unprecedented precision.

ACKNOWLEDGEMENTS

References

1. P. Gumbsch, in *Handbook of Materials Modeling,* ed. S. Yip (Dordrecht, Netherlands: Springer Verlag, 2005), pp. 2713–2718.
2. D. Raabe, F. Roters, F. Barlat, and L.-Q. Chen, editors, *Continuum Scale Simulation of Engineering Materials: Fundamentals–Microstructures–Process Applications* (Weinheim, Germany: Wiley-VCH, 2004).
3. G. Dehm, T.J. Balk, B. Von Blanckenhagen, P. Gumbsch, and E. Arzt, *Zeitschrift für Metallkunde,* 93 (2002), pp. 383–391.
4. B. Von Blanckenhagen, E. Arzt, and P. Gumbsch, *Acta Materialia,* 52 (2004), pp. 773–784.
5. J. Senger, D. Weygand, P. Gumbsch, and O. Kraft, *Scripta Materialia,* 58 (2008), pp. 587–590.
6. C. Motz, D. Weygand, J. Senger, and P. Gumbsch, *Acta Materialia,* 56 (2008), pp. 1942–1955.
7. D. Raabe and F. Roters, *Intern. J. Plast.,* 20 (2004), pp. 339–361.
8. E. Kröner, *Int. J. Solids and Structures,* 38 (2001), pp. 1115–1134.
9. T. Hochrainer, M. Zaiser, and P. Gumbsch, *Philosophical Magazine,* 87 (2007), pp. 1261–1282.
10. S. Sandfeld, T. Hochrainer, P. Gumbsch, and M. Zaiser, *Philosophical Magazine,* 90 (2010), pp. 3697–3728.
11. D. Raabe, P. Klose, B. Engl, K.-P. Imlau, F. Friedel, and F. Roters, *Adv. Eng. Mater.,* 4 (2002), pp. 169–180.
12. O. Engler and J. Hirsch, *Mat. Sci. Eng. A,* 336 (2002), pp. 249–262.

13. L. Neumann, R. Kopp, A. Ludwig, M. Wu, A. Bührig-Polaczek, M. Schneider, M. Crumbach, and G. Gottstein, *Mater. Sci. Eng.,* 12 (2004), pp. S19–S31.
14. N. Peranio, Y.J. Li, F. Roters, and D. Raabe, *Mater. Sc. Eng. A,* 527 (2010), pp. 4161–4168.
15 R. Song, D. Ponge, D. Raabe, J.G. Speer, and D.K. Matlock, *Mater. Sci. Eng. A,* 441 (2006), pp. 1–17.
16. P. Haupt, *Continuum Mechanics and Theory of Materials* (Berlin: Springer, 2002).
17. E. Kröner, "Allgemeine Kontinuumstheorie der Versetzungen und Eigenspannungen," *Archive for Rational Mechanics and Analysis,* 4 (1959), pp. 273–334.
18. J. Mandel, "Plasticite Classique et Viscoplasticite," CISM Course Vol. 97 (1971).
19. E. Lee and D. Liu, *J. Applied Physics,* 38 (1967), pp. 19–27.
20. A. Staroselsky and L. Anand, *Int. J. Plasticity,* 19 (2003), pp. 1843–1864.
21. S.R. Kalidindi, *J. Mechanics and Physics of Solids,* 46 (1998), pp. 267–271.
22. A. Prakash, S.M. Weygand, and H. Riedel, *Computational Materials Science,* 45 (3) (2009), pp. 744–750.
23. F. Roters, P. Eisenlohr, L. Hantcherli, D.D. Tjahjanto, T.R. Bieler, and D. Raabe, *Acta Mater.,* 58 (2010), pp. 1152–1211.
24. S. Turteltaub and A.S.J. Suiker, *J. Mechanics and Physics of Solids,* 53 (2005), pp. 1747–1788.
25. R.J. Asaro, in *Advances in Applied Mechanics Volume 23,* ed. John W. Hutchinson and Theodore Y. Wu (Amsterdam, the Netherlands: Elsevier, 1983), pp. 1–115.
26. A. Ma, F. Roters, and D. Raabe, *Acta Mater.,* 54 (2006), pp. 2169–2179.
27. J. Lubliner, *Plasticity Theory* (New York: Macmillan Publishing, 1990).
28. J.R. Rice, *J. Applied Mechanics,* 37 (1970), p. 728.
29. G. Cailletaud, O. Diard, F. Feyel, and S. Forest, *Technische Mechanik,* 23 (2003), pp. 130–145.
30. J.W. Hutchinson, *Proc. R. Soc. Lond. A,* 10 (348) (1976), pp. 101–127.
31. E. Voce, *J. Inst. Met.,* 74 (1948), pp. 537–562.
32. J. Harder, *Int. J. Plasticity,* 15 (1999), pp. 605–624.
33. M.E. Gurtin, *J. Mechanics and Physics of Solids,* 48 (2000), pp. 989–1036.
34. A. Ma, F. Roters, and D. Raabe, *Acta Mater.,* 54 (2006), pp. 2181–2194.
35. Z. Zhao, M. Ramesh, D. Raabe, A. Cuitino, and R. Radovitzky, *Int. J. Plast.,* 24 (2008), pp. 2278–2297.
36. F. Siska, S. Forest, and P. Gumbsch, *Computational Materials Science,* 39 (2007), pp. 137–141.
37. F. Siska, D. Weygand, S. Forest, and P. Gumbsch, *Computational Materials Science,* 45 (2009), pp. 793–799.
38. T.R. Bieler, P. Eisenlohr, F. Roters, D. Kumar, D.E. Mason, M.A. Crimp, and D. Raabe, *Int. J. Plast.,* 25 (2009), pp. 1655–1683.
39. E. Demir and D. Raabe, *Acta Mater.,* 58 (2010), pp. 6055–6063.
40. T. Walde, P. Gumbsch, and H. Riedel, *Steel Research International,* 77 (2006), pp. 741–746.
41. D. Raabe, Z. Zhao, S.-J. Park, and F. Roters, *Acta Mater.,* 50 (2002), pp. 421–440.
42. A. Reuss, *Z. Angew Math. Mech.,* 9 (1929), pp. 49–58.
43. W. Voigt, *Wied. Ann.,* 38 (1889), pp. 573–587.
44. G.L. Taylor, *J. Inst. Met.,* 62 (1938), pp. 307–324.
45. T.H. Lin, *J. Mechanics and Physics of Solids,* 5 (1957), pp. 143–149.
46. J.D. Eshelby, *Proc. Roy. Soc. Lond. A,* 241 (1957), pp. 376–396.

47. E. Kröner, *Z. Phys.,* 151 (1958), pp. 504–518.
48. T. Mori and K. Tanaka, *Acta Metall.,* 21 (1973), pp. 571–574.
49. R.A. Lebensohn and C.N. Tomé, *Acta Metall. et Mater.,* 41 (1993), pp. 2611–2624.
50. A. Prakash, T. Hochrainer, E. Reisacher, and H. Riedel, *Steel Research International,* 79 (2008), pp. 645–652.
51. M. Rodriguez Ripoll, E. Reisacher, and H. Riedel, *Computational Materials Science,* 45 (2009), pp. 788–792.
52. H. Wang, P.D. Wu, C.N. Tomé, and Y. Huang, *J. Mechanics and Physics of Solids,* 58 (2010), pp. 594–612.
53. P. Van Houtte, L. Delannay, and I. Samajdar, *Texture Microstruct.,* 31 (1999), pp. 109–149.
54. P. Van Houtte, S. Li, M. Seefeldt, and L. Delannay, *Int. J. Plast.,* 21 (2005), pp. 589–624.
55. C. Schäfer, J. Song, and G. Gottstein, *Acta Mater.,* 57 (2009), pp. 1026–1034.
56. P. Eisenlohr, D.D. Tjahjanto, T. Hochrainer, F. Roters, and D. Raabe, *Int. J. Materials Research,* 100 (2009), pp. 500–509.
57. T. Walde and H. Riedel, *Mater. Sci. and Eng. A,* 443 (2007), pp. 277–284.
58. I. Tikhovskiy, D. Raabe, and F. Roters, *Mater. Sci. Eng. A,* 488 (2008), pp. 482–490.
59. D. Raabe, M. Sachtleber, Z. Zhao, F. Roters, and S. Zaefferer, *Acta Mater.,* 49 (2001), pp. 3433–3441.
60. A.J. Beaudoin, H. Mecking, and U.F. Kocks, *Philos. Mag. A,* 73 (1996), pp.1503–1517.
61. M. Sachtleber, Z. Zhao, and D. Raabe, *Mater. Sci. Eng. A,* 336 (2002), pp. 81–87.
62. J. Ocenasek, M. Rodriguez Ripoll, S.M. Weygand, and H. Riedel, *Computational Materials Science,* 39 (2007), pp. 23–28.
63. R.A. Lebensohn, *Acta Mater.,* 49 (2001), pp. 2723–2737.
64. A. Prakash and R.A. Lebensohn, *Model. Sim. Mater. Sci. Eng.,* 17 (2009), 064010.
65. A. Butz, S. Lossau, B. Springub, and F. Roters, *Int. J. Mater. Forming,* 3 (Suppl. 1) (2010), pp. 73–76.
66. C. Yeong and S. Torquato, *Phys. Rev. E,* 57 (1998), pp. 495–506.
67. D. Raabe, *Ann. Rev. Mater. Res.,* 32 (2002), pp. 53–76.
68. F. Barlat and J. Lian, *Int. J. Plasticity,* 5 (1989), pp. 51–56.
69. S. Lossau and B. Svendsen, "Forming Simulations Based on Parameters Obtained in Microstructural Cold Rolling Simulations in Comparison to Conventional Forming Simulations" (Presented at the 7th LS-DYNA User Conference, Salzburg, Austria, 2009), C-I-01.
70. F. Feukamm, M. Feucht, A. Haufe, and K. Roll, *Proc. 7th Int. Conf. Numerical Simulation of 3D Sheet Metal Forming Processes* (Zurich Switzerland: ETH Zurich, Institute of Virtual Metallurgy, 2008), pp. 805–810.

Dirk Helm, Alexander Butz, and Peter Gumbsch are with Fraunhofer Institute for Mechanics of Materials IWM, Wöhlerstr. 11, 79108 Freiburg, Germany; Dierk Raabe is with Max-Planck-Institute for Iron Research, Max-Planck-Str. 1, 40237 Düsseldorf, Germany. Gumbsch is also with the Institute for Applied Materials IAM, Karlsruhe Institute of Technology KIT, Kaiserstraße 12, 6131 Karlsruhe, Germany. Dr. Helm can be reached at dirk.helm@iwm. fraunhofer.de.